Direct measurement of the resonance strengths and branching ratios of low-energy (p, γ) reactions on Mg isotopes*

Hao Zhang(张昊)[1] Zhi-Hong Li(李志宏)[1,2†] Jun Su(苏俊)[3] Yun-Ju Li(李云居)[1] Chen Chen(陈晨)[1]
Long Zhang(张龙)[1] Fu-Qiang Cao(曹富强)[1] Yang-Ping Shen(谌阳平)[1] Wei Nan(南巍)[1]
Wei-Ke Nan(南威克)[1] Xin-Yue Li(李鑫悦)[1,3] Li-Hua Chen(陈立华)[1] Gang Lian(连刚)[1]
Bao-Qun Cui(崔保群)[1] Bing Guo(郭冰)[1] Wei-Ping Liu(柳卫平)[1]

[1]China Institute of Atomic Energy, Beijing 102413, China
[2]University of Chinese Academy of Science, Beijing 101408, China
[3]Beijing Normal University, Beijing 100875, China

Abstract: Proton capture reactions on Mg isotopes are significant in the Mg-Al cycle in stellar H-burning. In particular, the resonance strengths and branching ratios of low-energy resonances in ^{25}Mg$(p,\gamma)^{26}$Al reactions determine the production of ^{26}Al, which is one of the most important long-lived radioactive nuclei in nuclear astrophysics. In this article, we report our first experiment using the intense proton beam of approximately 2 mA provided by the JUNA accelerator ground laboratory and a new technique that can minimize the composition change of targets under intense beam irradiation. The resonance strengths and branching ratios of E = 214, 304, and 326 keV resonances in the reactions of ^{24}Mg$(p,\gamma)^{25}$Al, ^{25}Mg$(p,\gamma)^{26}$Al, and ^{26}Mg$(p,\gamma)^{27}$Al, respectively, were measured with high accuracy. The success of this experiment provides a good calibration for the nuclear astrophysical experiment at the Jinping underground laboratory.

Keywords: stellar hydrogen burning, resonance reactions, radiative capture

DOI: 10.1088/1674-1137/ac06aa

I. INTRODUCTION

Based on the observation of 1.809 MeV γ-ray results from space detectors in the 1980s, a large amount (2–3 $M_\odot$) of radionuclide ^{26}Al has been proven to exist in the galaxy [1], which demonstrates that the nucleosynthesis processes of ^{26}Al is currently active. Since ^{26}Al has a half-life of 7.25×10^5 yr, we can infer that it was produced in a relatively recent age. Since the thermonuclear reactions that generate ^{26}Al require very high temperatures, the astrophysical sites that produced ^{26}Al should be explosive or in the convective environment of Wolf-Rayet stars, which can eject the ^{26}Al production into interstellar space. Today, the origin of ^{26}Al in the galaxy has become a popular topic in nuclear astrophysics.

Since the first observation of 1.809 MeV γ-rays by the HEAO-3 satellite in 1982 [2], many studies have achieved significant progress on this subject [3-11], and the results indicate that the main reaction to generate ^{26}Al is ^{25}Mg$(p,\gamma)^{26}$Al. The ground state of ^{26}Al will decay to the excited state of ^{26}Mg and the observed 1.809 MeV γ-ray results from the de-excitation process of the ^{26}Mg excited state. A short-lived isomeric state with a half life of 6.35 s occurs at E_x = 228 keV in ^{26}Al, which decays to the ground state of ^{26}Mg without emitting 1.809 MeV γ-rays. Therefore, the ground state fraction f_0 of the ^{25}Mg$(p,\gamma)^{26}$Al reaction must be considered in the study of interstellar ^{26}Al.

Interstellar ^{26}Al is primarily generated from Mg-Al reaction cycles of hydrogen burning in massive stars. The proton capture reaction of Mg isotopes is crucial in the reaction cycle. The (p,γ) reaction on Mg is dominated by narrow resonances in the energy range from 50 to 350 keV. Their resonance strengths should be determined precisely in experiments to study their contribution to the interstellar ^{26}Al production.

In this article, we report the direct measurements of ^{24,25,26}Mg(p,γ) reactions using the newly designed JUNA accelerator [12]. The resonance strengths and branching ratios of the E = 214 keV resonance in ^{24}Mg$(p,\gamma)^{25}$Al, E = 304 keV resonance in ^{25}Mg$(p,\gamma)^{26}$Al, and E = 326 keV resonance in ^{26}Mg$(p,\gamma)^{27}$Al at the ground laboratory

Received 17 April 2021; Accepted 31 May 2021; Published online 2 July 2021

* Supported by the National Natural Science Foundation of China (11490563, 11961141003) and the Continuous Basic Scientific Research Project (WDJC-2019-13)

† E-mail: zhli@ciae.ac.cn

are measured. The experimental results provide references for Jinping deep underground experiments.

II. EXPERIMENTAL SETUP

The experiment was conducted on the newly built high-current 400 kV accelerator [13] for the JUNA experiment, which was designed and manufactured at the China Institute of Atomic Energy in Beijing. The JUNA accelerator can supply high ion beams of H^+ and He^+ with a high current of 10 mA, or He^{2+} of 2 mA, for which the maximum energy is doubled to 800 keV. In this experiment, the proton capture reaction on magnesium isotopes was measured in the energy range of E_p = 220 - 400 keV. The experimental setup is shown in Fig. 1. The proton beam focused on the water-cooled target after passing through two collimators with diameters of 12 and 8 mm, respectively. A copper pipe was placed in front of the target and cooled using LN_2 to minimize the carbon deposition on the target surface. A negative voltage of 300 V was applied to the copper pipe to gather the secondary electrons from the target. The voltage was optimized to obtain a maximum beam current.

Compared with the traditional solid targets, the targets used in this experiment were improved by covering a Cr protective layer over the surface of the evaporated Mg targets. Cr is the hardest metal in nature. It oxidizes slowly and can protect a target when plated over its surface. Since the atomic number of Cr is significantly larger than that of Mg, the cross section of proton capture on Cr can be negligible compared with Mg. First, natural metal Mg was evaporated onto a 3 mm thick copper [14] to create an Mg target with a thickness of 40 μg/cm^2. A Cr layer of 23 nm was then sputtered on the surface of the Mg target. This Cr-Mg-Cu structure target can effectively reduce the radiation damage, as indicated in Refs. [15, 16]. The radiation damage manifested as a change in the composition of the target and thus increased the uncertainty of the experimental results. For a narrow resonance reaction with consistent experimental conditions, the maximum yield is proportional to the effective stopping power; therefore, it is only related to the composition of the target. Figure 2 shows the yield plateau of the ^{25}Mg$(p,\gamma)^{26}$Al reaction at the E = 304 keV resonance

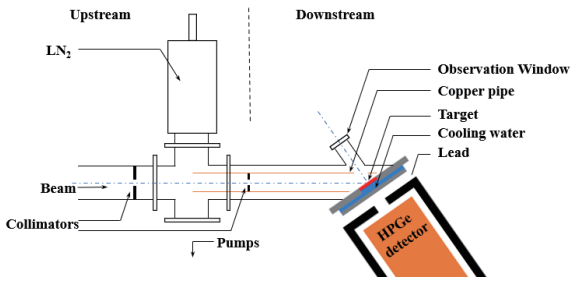

Fig. 1. (color online) Schematic of the experimental setup.

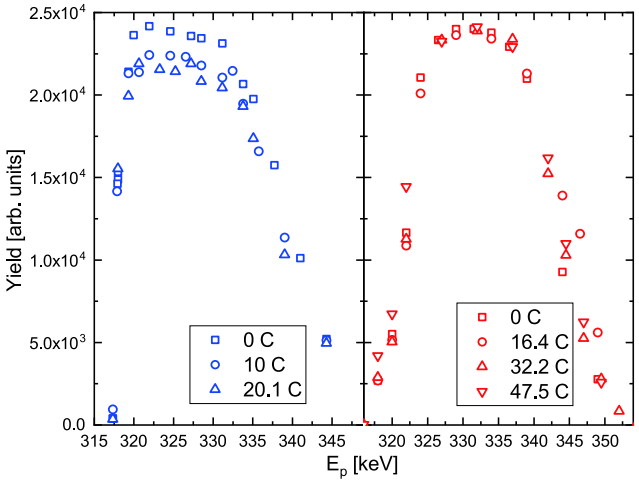

Fig. 2. (color online) Yield curves obtained for the E = 304 keV resonance of ^{25}Mg$(p,\gamma)^{26}$Al for the Mg target (left) and Cr-coated Mg target (right). The squares, circles, and triangles on the left represent the scan of the Mg target without a Cr layer after bombardment with 0, 10, and 20.1 C proton beams, and the squares, circles, positive triangles, and inverted triangles on the right represent the scan of the Cr-coated Mg target after bombardment with 0, 16.4, 32.2, and 47.5 C proton beams, respectively.

with and without a Cr protective layer. The composition of the target with a Cr layer remained basically unchanged under the radiation of 47.5 C proton beams, while the maximum yields of the target without a Cr layer decreased by approximately 10% under the radiation of 20.1 C proton beams. The protected target exhibited high durability against intense beams in the experiment to measure the low cross-section reaction.

The γ-ray spectra of this experiment were measured using an HPGe detector with a relative efficiency of 175% and a resolution of 2.1 keV at E_γ = 1.3 MeV. The detector was placed at 55° with respect to the relative beam direction parallel to the target, the distance between the detector and the target was 25 cm, and the summing-effect was less than 1%. The detector was shielded with 5 cm thick lead planks, and the background could be reduced by almost an order of magnitude.

The absolute efficiency of the HPGe detector was determined using a ^{56}Co γ-ray source with an uncertainty of 1%. For high-energy γ-rays, the efficiency was calibrated using resonances of well-studied reactions, an E = 259 keV resonance of ^{14}N$(p,\gamma)^{15}$O [17] and E = 315 keV resonance of ^{27}Al$(p,\gamma)^{28}$Si [18]. The calibration encompassed an energy range from 0.8 to 10.1 MeV. The maximum γ-ray energy of the Mg isotope was 8.6 MeV, and all γ-rays from proton capture reactions on Mg isotopes were within the range of the energy calibration. In the calibration experiment, a TiN target and metal Al target produced through magnetron sputtering were bombarded with a proton beam of 300 μA. The efficiencies obtained

by the reactions were determined from the known branching ratios and resonance strengths. Figure 3 shows the results of the absolute efficiencies of the HPGe detector. The uncertainties were primarily due to the uncertainty of the statistics, as well as the branching ratios and resonance strengths from ^{14}N$(p,\gamma)^{15}$O [17] and ^{27}Al$(p,\gamma)^{28}$Si [18] reactions. We also performed a Geant4 [19] simulation for the experimental setup, and the simulation results agreed closely with the experimental data within a 1% difference, and the total efficiency uncertainty was approximately 2%, deduced from the weighted average of all the experimental data.

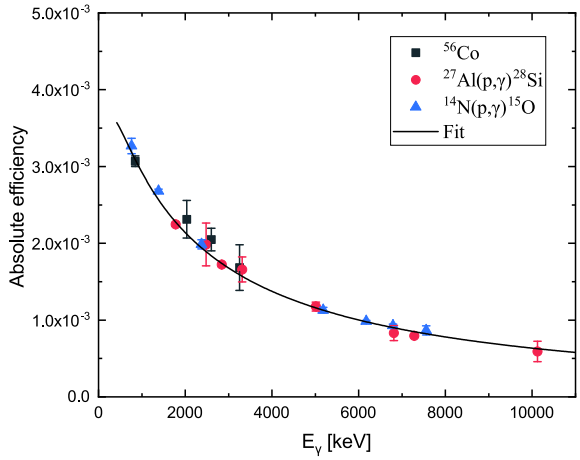

Fig. 3. (color online) Absolute efficiency determined for the HPGe detector using a ^{56}Co γ-ray source (squares), ^{14}N$(p,\gamma)^{15}$O (positive triangles), and ^{27}Al$(p,\gamma)^{28}$Si (circles). The solid curve denotes the fitted values of experimental data.

III. MEASUREMENT AND RESULTS

For a narrow resonance, the absolute resonance strength of the (p,γ) reaction is determined by the maximum thick-target yield $Y_{\max}$, according to [20]

$$Y_{\max} = \frac{\lambda^2}{2} b_\gamma \omega\gamma \frac{m_{\rm Mg} + m_p}{m_{\rm Mg}} \frac{1}{\varepsilon_{\rm eff}} \varepsilon(E_\gamma), \quad (1)$$

where λ, b_γ, $\omega\gamma$, $m_{\rm Mg}$, m_p, $\varepsilon_{\rm eff}$, and $\varepsilon(E_\gamma)$ represent the de Broglie wavelength at the resonance energy, branching ratio, resonance strength, masses of magnesium and proton, effective stopping power, and absolute efficiency at E_γ, respectively. Considering the main components of the target, the effective stopping power of Mg targets is expressed by

$$\varepsilon_{\rm eff} = \frac{1}{X_{\rm Mg}} \left(\varepsilon_{\rm Mg} + \frac{N_{\rm O}}{N_{\rm Mg}} \varepsilon_O \right), \quad (2)$$

where $X_{\rm Mg}$ is the relative isotopic abundance of stable magnesium isotope, and $N_{\rm O}$ and $N_{\rm Mg}$ are the number densities of oxygen and magnesium in the target, respectively. The values of $\varepsilon_{\rm Mg}$, $\varepsilon_{\rm O}$, and $X_{\rm Mg}$ are provided in Refs. [21, 22].

Evaporated Mg targets are expected to consist of a pure layer of magnesium; however, these targets are known to consist of the compound Mg_5O owing to oxidization during target preparation [23]. In this study, the $N_{\rm O}/N_{\rm Mg}$ ratio was determined to be 21.3±2.0% by measuring the yield of the E = 189 keV resonance in the ^{25}Mg$(p,\gamma)^{26}$Al reaction [16] and E = 143 keV resonance in the ^{18}O$(p,\gamma)^{19}$F reaction [24] simultaneously using a 4π BGO detector array and a 150 μg/cm^2 ^{25}Mg target. The BGO detector was composed of eight identical BGO segments, each with a length of 25 cm and a radial thickness of 6.3 cm, covering a 45° azimuthal angle. The summing efficiency and energy resolution of the BGO array were 60% and 4% at 7 MeV under the temperature of −10 °C. As shown in Fig. 4, the summing energy spectrum of the ^{25}Mg$(p,\gamma)^{26}$Al (E_γ = 6.5 MeV) and ^{18}O$(p,\gamma)^{19}$F (E_γ = 8.1 MeV) reactions were reproduced using the Geant4 simulation. The uncertainties for the $N_{\rm O}/N_{\rm Mg}$ ratio (~ 10%) were due to the uncertainties of the resonance strengths of ^{18}O$(p,\gamma)^{19}$F (~ 6.5%) and ^{25}Mg$(p,\gamma)^{26}$Al (~ 6.7%), the geometric uncertainties of the BGO detector simulations (~ 4%), and statistics (~ 1%). The ratio supported the Mg_5O structure of the target. Using the ratio and the abundance data, the effective stopping power values for proton in ^{24}Mg, ^{25}Mg, and ^{26}Mg target at the resonance energies were deduced to be 22.3, 151.7, and 133.4 eV cm^2 10^{-15} atoms, respectively. The uncertainties (~ 3.7%) of these values resulted from the stopping power uncertainties (~ 3.9%) [21] and the $N_{\rm O}/N_{\rm Mg}$ ratio (~ 10%).

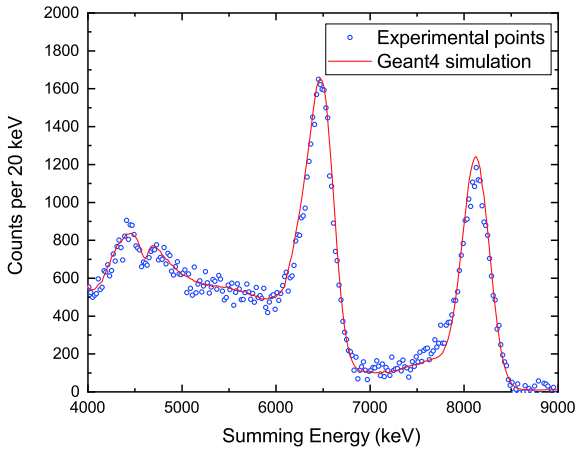

Fig. 4. (color online) γ-ray spectrum captured using a BGO detector at E = 189 keV resonance of ^{25}Mg$(p,\gamma)^{26}$Al reaction (E_γ = 6.5 MeV) and E = 143 keV resonance of ^{18}O$(p,\gamma)^{19}$F reaction (E_γ = 8.1 MeV). The blue dots and solid red line represent the measurement and Geant4 simulation, respectively.

The ^{24}Mg$(p,\gamma)^{25}$Al, ^{25}Mg$(p,\gamma)^{26}$Al and ^{26}Mg$(p,\gamma)^{27}$Al reactions were measured at E_p = 242, 330, and 354 keV, respectively, over an minimum charge integration of 10 C using a proton beam of approximately 2 mA. The γ-ray spectra of the measurements are shown in Figs. 5, 6, 7. The triple-line γ-ray sets in the figures denote the full-energy, single-escape, and double-escape peaks. Since the reaction yields measured in this experiment were relatively large, both resonance strength and branching ratio were accurately obtained even at a distance of 25 cm. Some natural and beam-induced γ-ray lines can be observed in the figures, such as ^{40}K, ^{208}Tl, and the reactions of ^{13}C$(p,\gamma)^{14}$N and ^{19}F$(p,\alpha\gamma)^{16}$O. They resulted from the adsorption of air by the target and reagent of the machining. These peaks had a slight effect in obtaining resonance strengths and branching ratios because of the high energy resolution of the HPGe detector. The dead time rate was less than 5%, which was corrected in the data analysis. In the measurement, the target composition was established with the yields of ^{24}Mg$(p,\gamma)^{25}$Al at E = 214 keV before and after the measurement.

The branching ratio of the primary γ-rays in the reactions can be calculated using

$$b_\gamma(i) = \frac{Y_i/\varepsilon(E_{\gamma_i})}{\sum_i Y_i/\varepsilon(E_{\gamma_i})}, \tag{3}$$

where Y_i is the yield for the ith γ-ray, and $\varepsilon(E_{\gamma_i})$ is the absolute efficiency of the corresponding primary γ-rays.

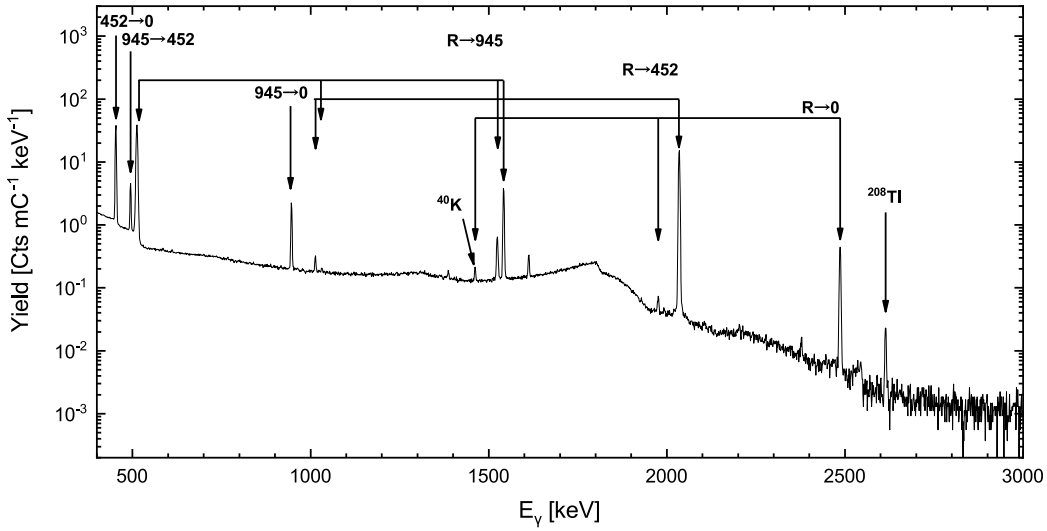

Fig. 5. HPGe γ-ray spectra of ^{24}Mg$(p,\gamma)^{25}$Al at E = 214 keV with accumulated proton beam of 12 C. All the primary transitions and secondary transitions are labeled.

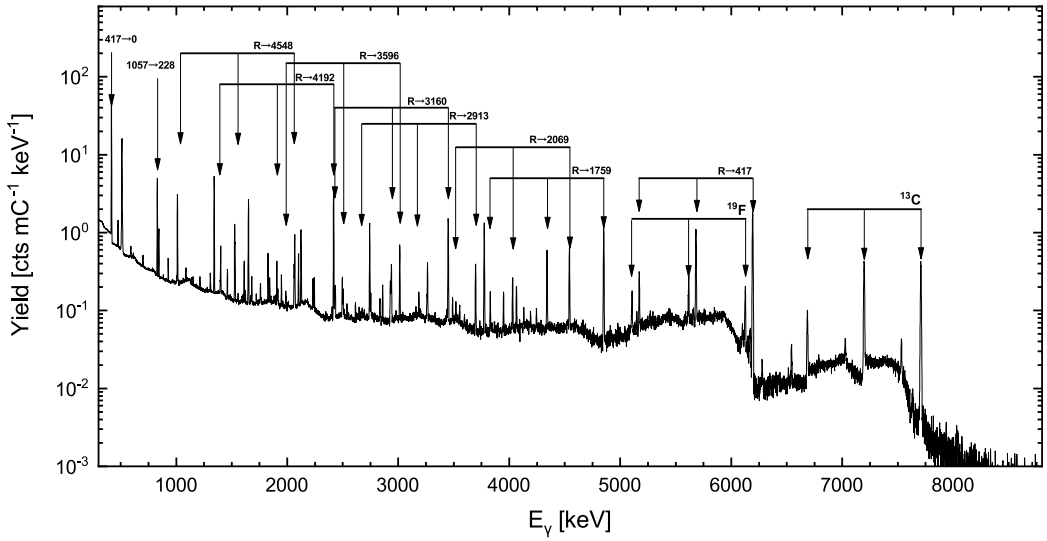

Fig. 6. HPGe γ-ray spectra of ^{25}Mg$(p,\gamma)^{26}$Al captured at the E = 304 keV using an accumulated proton beam of 16 C. The primary transitions with a branching ratio greater than 2% and two important secondary transitions (417 → 0 and 1057 → 228) are labeled.

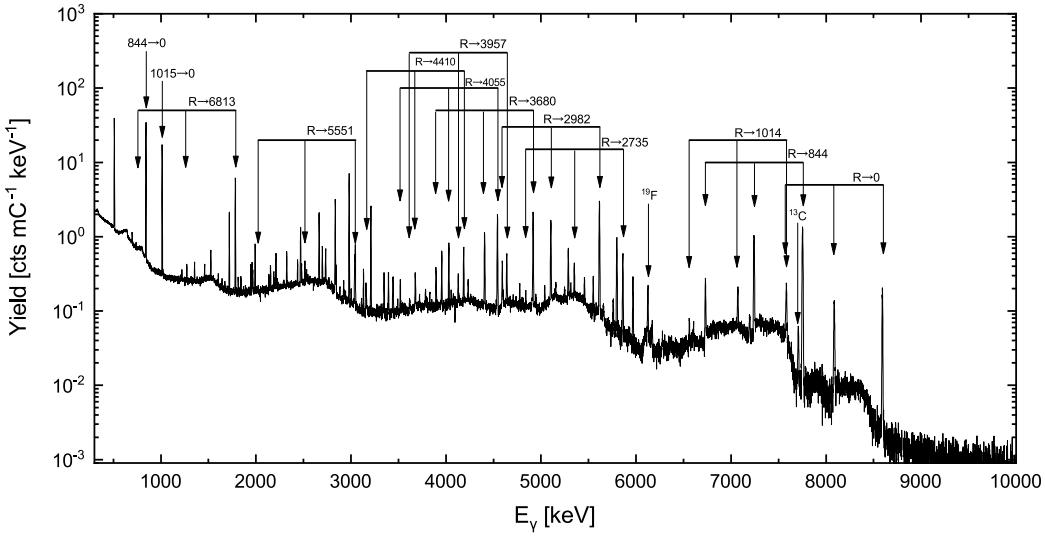

Fig. 7. The HPGe γ-ray spectra of ^{26}Mg$(p,\gamma)^{27}$Al at E = 326 keV using an accumulated proton beam of 10 C. The primary transitions with a branching ratio greater than 2% and an important secondary transition 844 → 0 are labeled.

The level energies for the compound nuclei were referenced from level diagrams of online nuclear data at the NNDC [25]. The peak area was extracted by fitting the spectra with a Gaussian distribution and linear background, and it was then used to determine the total yields with the Geant4 simulation. For the very weak and overlapped γ-ray lines, the simulation results were used to obtain the peak areas. By analyzing the energy spectra of three proton capture reactions on Mg target, the branching ratios for the ^{24}Mg$(p,\gamma)^{25}$Al, ^{25}Mg$(p,\gamma)^{26}$Al, and ^{26}Mg$(p,\gamma)^{27}$Al reactions were extracted and listed as given in Tables 1, 2, and 3, together with other existing results. The results of this study were in agreement with the data from Refs. [15, 23, 26]. The ground state fraction f_0 of the ^{25}Mg$(p,\gamma)^{26}$Al reaction at 304 keV resonance was determined to be 85.9 ±1.0% using our study's primary γ-ray branching ratio and the cascade branching ratio data from NNDC [25]. The value agreed with the value of Limata *et al*., (87.8 ±1.2%) [15], and this indicated a more ^{26}Al isomeric state production in the stellar Mg-Al reaction cycle.

Using the branching ratios determined in this study, the absolute resonance strengths $\omega\gamma$ could be obtained from the maximum thick-target yield using Eq. (1). The resonance strengths of E = 214 keV in ^{24}Mg$(p,\gamma)^{25}$Al, E = 304 keV in ^{25}Mg$(p,\gamma)^{26}$Al and E = 326 keV in ^{26}Mg$(p,\gamma)^{27}$Al determined in this and other studies are listed in Table 4. The uncertainties of the our results were due to the uncertainties in the statistics (~ 1%) in HPGe measurement, efficiency calibration (~ 2%), effective stopping power (~ 3.7%), and charge integration (~ 2%).

Table 1. Primary γ-ray branching ratios of the ^{24}Mg$(p,\gamma)^{25}$Al E = 214 keV resonance from this and previous studies.

E_x	This study	[15]	[26]
1790		<0.05	<0.8
1613		<0.05	<0.8
945	15.8 ± 0.2	15.6 ± 0.3	15.6 ± 1.1
452	81.5 ± 1.2	81.7 ± 1.6	81.7 ± 3.4
0	2.77 ± 0.06	2.70 ± 0.07	2.7 ± 0.3

For the E = 214 keV resonance in the ^{24}Mg$(p,\gamma)^{25}$Al reaction, the $\omega\gamma$ = 11.5 ± 0.5 meV was determined in this study, and the value was in agreement with the data from the previous studies [15, 26-28]. We recommend a resonance strength of $\omega\gamma$ = 11.3 ± 0.5 meV for the ^{24}Mg$(p,\gamma)^{25}$Al 214 keV resonance using the method of weighted average [29]. The resonance strength of ^{25}Mg$(p,\gamma)^{26}$Al at E = 304 keV was determined to be 31.2 ± 1.5 meV, which closely agreed with the NACRE value [28] and the results reported in Refs. [15, 23, 30, 31] but with a small uncertainty. Based on the results, we recommended a value of $\omega\gamma$ = 31.0 ± 1.0 meV for the resonance strength. For the resonance strength of E = 326 keV in ^{26}Mg$(p,\gamma)^{27}$Al, this study indicated a resonance strength of $\omega\gamma$ = 279 ± 13 meV, which was consistent with the value reported in Refs. [15, 32] within error bars but much smaller than the earlier NACRE compilation value [28] from the very earlier studies [23, 33-37]. Therefore, after discarding the questionable threefold higher values [34-37], we recommend a resonance strength of $\omega\gamma$ = 274 ± 8 meV for the ^{26}Mg$(p,\gamma)^{27}$Al 326 keV resonance.

IV. CONCLUSIONS

In this study, we precisely measured the resonance strengths and branching ratios for the reactions ^{24}Mg$(p,\gamma)^{25}$Al, ^{25}Mg$(p,\gamma)^{26}$Al, and ^{26}Mg$(p,\gamma)^{27}$Al at 214,

Table 2. Primary γ-ray branching ratios of the ^{25}Mg(p, γ)^{26}Al E = 304 keV resonance from this and previous studies.

E_x	This study	[15]	[23]
5916	0.07 ± 0.02	0.09 ± 0.02	
5726	0.09 ± 0.02	0.10 ± 0.01	0.12 ± 0.03
5457	0.15 ± 0.06		
5396	0.24 ± 0.03	0.22 ± 0.02	0.35 ± 0.05
4940	0.12 ± 0.07	0.08 ± 0.01	
4622	0.27 ± 0.11	0.28 ± 0.07	0.38 ± 0.06
4599	0.11 ± 0.03	0.12 ± 0.01	0.13 ± 0.04
4548	1.26 ± 0.08	1.30 ± 0.07	2.0 ± 0.1
4349		0.03 ± 0.01	
4206	0.18 ± 0.04	0.25 ± 0.02	0.25 ± 0.05
4192	18.9 ± 0.3	19.1 ± 0.3	14.7 ± 0.8
3963	0.18 ± 0.03	0.17 ± 0.01	0.12 ± 0.05
3750	0.90 ± 0.05	0.92 ± 0.02	1.5 ± 0.1
3681	1.02 ± 0.05	1.09 ± 0.03	0.71 ± 0.08
3675	0.92 ± 0.13	0.86 ± 0.13	0.59 ± 0.06
3596	4.31 ± 0.20	4.29 ± 0.07	3.3 ± 0.2
3160	11.3 ± 0.05	11.4 ± 0.2	15.6 ± 0.9
3073	0.13 ± 0.05	0.11 ± 0.04	0.08 ± 0.05
2913	3.07 ± 0.14	3.04 ± 0.05	4.2 ± 0.3
2661	1.06 ± 0.06	1.00 ± 0.02	1.6 ± 0.1
2545	1.45 ± 0.03	1.46 ± 0.03	0.9 ± 0.1
2365	0.37 ± 0.05	0.47 ± 0.02	0.27 ± 0.07
2068.9	6.3 ± 0.1	6.0 ± 0.1	6.5 ± 0.4
1759	15.80 ± 0.3	16.1 ± 0.3	22.7 ± 1.3
417	31.71 ± 0.4	31.8 ± 0.5	24 ± 1.4
0		0.058 ± 0.004	

Table 3. Primary γ-ray branching ratios of the ^{26}Mg(p, γ)^{27}Al E = 326 keV resonance from this and previous studies.

E_x	This study	[15]	[23]
7858	0.08 ± 0.03	0.09 ± 0.02	0.17 ± 0.03
7280		<0.01	0.03 ± 0.01
7071	0.51 ± 0.04	0.30 ± 0.02	0.25 ± 0.02
6993	0.15 ± 0.02	0.17 ± 0.02	0.20 ± 0.02
6813	12.04 ± 0.13	12.1 ± 0.1	12.6 ± 0.7
6776	0.06 ± 0.02	0.06 ± 0.01	0.06 ± 0.02
6651	0.47 ± 0.02	0.45 ± 0.02	0.50 ± 0.04
6605	1.31 ± 0.03	1.26 ± 0.03	1.41 ± 0.09
6158	0.65 ± 0.03	0.71 ± 0.03	0.72 ± 0.05
6116	0.46 ± 0.02	0.44 ± 0.02	0.34 ± 0.04
6081	0.57 ± 0.03	0.59 ± 0.03	0.55 ± 0.05
5752	0.79 ± 0.05	0.80 ± 0.03	0.89 ± 0.06
5551	2.15 ± 0.05	2.07 ± 0.05	0.39 ± 0.03
5438	0.39 ± 0.04	0.22 ± 0.03	0.52 ± 0.04
5248	0.90 ± 0.04	0.94 ± 0.03	0.95 ± 0.06
5156	0.72 ± 0.03	0.71 ± 0.03	0.03 ± 0.02
4812	0.35 ± 0.02	0.54 ± 0.03	0.59 ± 0.05
4410	2.86 ± 0.09	2.96 ± 0.07	3.1 ± 0.2
4055	10.90 ± 0.1	10.9 ± 0.2	10.7 ± 0.6
3957	2.62 ± 0.07	2.64 ± 0.07	2.6 ± 0.2
3680	13.43 ± 0.2	14.5 ± 0.2	13.9 ± 0.8
2982	21.26 ± 0.2	19.7 ± 0.3	20.2 ± 0.1
2735	4.52 ± 0.1	4.43 ± 0.09	4.3 ± 0.3
1014	2.37 ± 0.1	2.04 ± 0.07	2.3 ± 0.2
844	18.28 ± 0.2	19.3 ± 0.3	20.2 ± 0.1
0	2.15 ± 0.04	2.06 ± 0.05	2.5 ± 0.2

Table 4. Absolute resonances strengths of proton capture reaction in magnesium isotopes.

Reactions	E_R/keV	$\omega\gamma$/meV						
		Present work	[15]	[28]	[23]	[32]	[26]	Recommendation
^{24}Mg(p,γ)^{25}Al	214	11.5 ± 0.5	10.6 ± 0.6	10 ± 2			12.7 ± 0.9	11.3 ± 0.5
^{25}Mg(p,γ)^{26}Al	304	31.2 ± 1.5	30.7 ± 1.7	31 ± 2	30 ± 4			31.0 ± 1.0
^{26}Mg(p,γ)^{27}Al	326	279 ± 13	274 ± 15	590 ± 10	250 ± 30	273 ± 13		274 ± 8

304, and 326 keV, respectively, using the newly built JUNA accelerator at the ground laboratory. Through the protection of a Cr layer sputtered on the surface of Mg target, the radiation protection capability of the target was significantly improved. This avoided the change in target composition caused by radiation and reduced the experimental uncertainties. Compared with previous experiments, we increased the precision of the resonance strengths.

The success of this experiment has provided an overall systematic calibration for the planned underground JUNA experiment. We also present the recommended resonance strengths of 11.3 ± 0.5 meV for the ^{24}Mg(p,γ)^{25}Al reaction at E = 214 keV, 31.0 ± 1.0 meV for the ^{25}Mg(p,γ)^{26}Al reaction at E = 304 keV, and 274 ± 8 meV for the ^{26}Mg(p,γ)^{27}Al reaction at 326 keV based on the results of this and other recent studies. The results provide more accurate inputs for the Mg-Al cycle net-

work calculations. In the near future, the direct measurement of resonance strength of 92 and 189 keV in the ^{25}Mg$(p,\gamma)^{26}$Al proton capture reaction will be performed by using the underground JUNA accelerator.

References

[1] R. Diehl, H. Halloin, K. Kretschmer *et al*., Nature **439**, 45 (2006)
[2] W. A. Mahoney, J. C. Ling, A. S. Jacobson *et al*., Astrophys. J. **262**, 742 (1982)
[3] M. Guélin, M. Forestini, P. Valiron *et al*., Astron. Astrophys. **297**, 183 (1995)
[4] G. H. Share, R. L. Kinzer, J. D. Kurfess *et al*., Astrophys. J. **292**, L61 (1985)
[5] G. H. Share, R. L. Kinzer, J. D. Kurfess *et al*., Astrophys. J. **326**, 717 (1988)
[6] P. von Ballmoos, R. Diehl, and V. Schönfelder, Astrophys. J. **318**, 654 (1987)
[7] P. Von Ballmoos, Astrophys. J. **380**, 98 (1991)
[8] D. Smith, R. P. Lin, P. Feffer *et al*., Astron. Astrophys. Suppl. Ser. **97**, 199 (1993)
[9] C. J. Maccallum, A. F. Huters, P. D. Stang *et al*., Astrophys. J. **317**, 877 (1987)
[10] Z. H. Li, J. Su, Y. J. Li *et al*., Sci China-Phys Mech Astron **58**(8), 082002 (2015)
[11] Y. J. Li, Z. H. Li, E. T. Li *et al*., Phys. Rev. C **102**, 025804 (2020)
[12] W. P. Liu, Z. H. Li, J. J. He *et al*., Sci China-Phys. Mech. Astron. **59**, 642001 (2016)
[13] Q. Wu, Y.G. Liu, J.L. Liu *et al*., J. Instrum. **14**, C02009 (2019)
[14] C. Chen, Y. J. Li, H. Zhang *et al*., Nucl. Sci. Tech. **31**, 91 (2020)
[15] B. Limata, F. Strieder, A. Formicola *et al*., Phys. Rev. C **82**, 015801 (2010)
[16] F. Strieder, B. Limata, A. Formicola *et al*., Phys. Lett. B **707**, 60 (2012)
[17] S. Daigle, K. J. Kelly, A. E. Champagne *et al*., Phys. Rev. C **94**, 025803 (2016)
[18] S. Harissopulos, C. Chronidou, K. Spyrou *et al*., Eur. Phys. J. A **9**, 479 (2000)
[19] S. Agostinelli *et al*. (Geant4 Collaboration), Nucl. Instr. Meth. A **506**, 250 (2003)
[20] C. Rolfs and W. S. Rodney, Cauldrons in the Cosmos (University of Chicago Press, Chicago, 1988)
[21] J. F. Ziegler, M. D. Ziegler b, and J.P. Biersack, Nucl. Instrum. Methods B **268**, 1818 (2010)
[22] T. B. Coplen, J. K. Böhlke, P. D. Bièvre *et al*., Pure Appl. Chem. **74**, 1987 (2002)
[23] C. Iliadis, T. Schange, C. Rolfs *et al*., Nucl. Phys. A **512**, 509 (1990)
[24] R.B. Vogelaar, T.R. Wang, S.E. Kellogg *et al*., Phys. Rev. C **42**, 753 (1990)
[25] M. S. Basunia and A. M. Hurst, Nucl. Data Sheets **134**, 1 (2016)
[26] D. C. Powell, C. Iliadis, A. E. Champagne *et al*., Nucl. Phys. A **660**, 349 (1999)
[27] H. P. Trautvetter and C. Rolfs, Nucl. Phys. A **242**, 519 (1975)
[28] C. Angulo, M. Arnould, M. Rayet *et al*., Nucl. Phys. A **656**, 3 (1999)
[29] R. Taylor, An Introduction To Error Analysis (University Science Books, Sausalito California, 1982)
[30] A. E. Champagne, A. J. Howard, and P. D. Parker, Nucl. Phys. A **402**, 179 (1983)
[31] P. M. Endt, P. de Wit, and C. Alderliesten, Nucl. Phys. A **459**, 61 (1986)
[32] D. C. Powell, C. Iliadis, A. E. Champagne *et al*., Nucl. Phys. A **644**, 263 (1998)
[33] L. Buchmann, H. W. Becker, K. U. Kettner *et al*., Z. Phys. A **296**, 273 (1980)
[34] C. Vanderleun, P. Endt, J. Kluyver *et al*., Physica **22**, 1223 (1956)
[35] C. Vanderleun and P. Endt, Physica **29**, 990 (1963)
[36] J. Keinonen and S. Brandenburg, Nucl. Phys. A **341**, 345 (1980)
[37] J. J. A. Smit, J. P. L. Reinecke, M. A. Meyer *et al*., Nucl. Phys. A **377**, 15 (1982)